Таблица 2 – Сводная статистика E_a и ln$A$ (100 итераций Монте-Карло)

Var	$\bar{x}$	σ	*min*	*max*	*Med*	*Sk*	*Kurt*
Модель A2							
E_a, кДж·моль$^{-1}$	26.69	0.30	26.04	27.45	26.69	0.10	–0.15
lnA, мин$^{-1}$	0.742	0.13	0.48	1.13	0.78	0.10	–0.10
Модель A3							
E_a, кДж·моль$^{-1}$	30.56	2.41	24.41	36.92	30.68	0.15	–0.10
ln A, мин$^{-1}$	–0.97	1.03	–3.63	1.72	-0.90	0.16	–0.07
Модель D3							
E_a, кДж·моль$^{-1}$	43.24	0.91	41.44	45.52	43.18	0.29	–0.18
lnA, мин$^{-1}$	13.87	0.42	13.06	14.94	13.84	0.33	–0.11

Список использованной литературы

1. Жуманазарова Г. М., Наукенова Е. Б., Байғонысова С., Арызқұлова А., Жайлау Е., Сарсенбекова А. Ж. Исследование кинетики термического распада сополимеров // Вестник КГИУ. – 2025. – № 2 (49).
2. Макашева С. Д., Советбекова А. Б., Кан А. Ж., Сарсенбекова А. Ж., Керуенбаева Ф. С., Жуманазарова Г. М. Кинетика и моделирование термического разложения: метод ABS и полиномиальная аппроксимация // Вестник КГИУ. – 2025. – № 2 (49).
3. Sarsenbekova A. Zh., Zhumanazarova G. M., Yildirim E., Tazhbayev Y. M., Kudaibergen G. K. RAFT agent effect on graft poly(acrylic acid) to polypropylene glycol fumarate phthalate / A. Zh. Sarsenbekova, G. M. Zhumanazarova, E. Yildirim, Y. M. Tazhbayev, G. K. Kudaibergen // Chemical Papers. – 2024. – Vol. 78. – P. 3831–3843. [На англ. языке].
4. Sarsenbekova A. Zh., Zhumanazarov G. M., Abulyaissov L. K., Figurinene I. V., Zhaslan R. K. et al. Study of mathematical models describing the thermal decomposition of polymers using numerical methods / A. Zh. Sarsenbekova, G. M. Zhumanazarov, L. K. Abulyaissov, I. V. Figurinene, R. K. Zhaslan et al. // Polymers. – 2025. – Vol. 17. – № 9. – P. 1197. [На англ. языке].
5. Sarsenbekova A. Zh., Burkeev M. Zh., Zhumanazarova G. M., Kudaibergen G. K., Nasikhatuly E. et al. The effect of liquid active media on the character of equilibrium swelling of copolymers based on polypropylene fumarate phthalate with acrylic acid / A. Zh. Sarsenbekova, M. Zh. Burkeev, G. M. Zhumanazarova, G. K. Kudaibergen, E. Nasikhatuly et al. // Eurasian Journal of Chemistry. – 2023. – Vol. 109, № 1. – P. 51–58. [На англ. языке].
6. Sarsenbekova A. Zh., Bolatbay A. N., Havlicek D., Issina Zh. A., Kabdenova N. A. et al. Effect of heat treatment on the supramolecular structure of copolymers based on poly(propylene glycol fumarate phthalate) with acrylic acid / A. Zh. Sarsenbekova, A. N. Bolatbay, D. Havlicek, Zh. A. Issina, N. A. Kabdenova et al. // Eurasian Journal of Chemistry. – 2024. – Vol. 29, № 2(114). – P. 61–73. [На англ. языке].
7. Ролингс Дж., Пантула С. Г., Дики Д. А. Прикладной регрессионный анализ: инструмент исследования / Дж. Ролингс, С. Г. Пантула, Д. А. Дики. – New York : Springer, 2001. – 440 с.
8. Seber G. A. F., Wild C. J. Nonlinear Regression / G. A. F. Seber, C. J. Wild. – Hoboken : Wiley, 2003. – 800 p. [На англ. языке].
9. Джеймс Г., Виттен Д., Хасти Т., Тибширани Р. Введение в статистическое обучение / Г. Джеймс, Д. Виттен, Т. Хасти, Р. Тибширани. – New York : Springer, 2013. – 426 с.
10. Монтгомери Д. С., Рангер Дж. С. Прикладная статистика и теория вероятностей для инженеров / Д. С. Монтгомери, Дж. С. Рангер. – 7-е изд. – Hoboken : Wiley, 2018. – 816 с. [На англ. языке].

UDC 538.9; 535.215; 539.23; 535.3

MODIFICATION OF ZnO ELECTRON TRANSPORT LAYER WITH TUNGSTEN DISELENIDE NANOPARTICLES FOR ORGANIC SOLAR CELLS

Seisembekova T.E., Karaganda Buketov University, Scientific Center for Nanotechnology and Functional Nanomaterials, Karaganda, Kazakhstan,

Kelgali G.K., Karaganda Buketov University, Scientific Center for Nanotechnology and Functional Nanomaterials, Karaganda, Kazakhstan,

Introduction

Zinc oxide ZnO is a promising material with applications not only in solar cells but also in other fields, such as UV photodetectors [1, 2], UV lasers [3], gas sensors [4], and photocatalytic water splitting [5]. ZnO is a wide-bandgap n-type semiconductor with intrinsic doping attributed to the presence of shallow donor levels [6]. However, achieving stable p-type

doping remains a challenge, as acceptor impurities in ZnO predominantly form deep levels rather than shallow acceptor states [6].

Due to its wide bandgap and high charge carrier mobility, ZnO holds significant potential for applications in optoelectronics and photovoltaics. However, its performance is limited by the high carrier recombination rate and insufficient photogeneration. The incorporation of transition metal dichalcogenides, such as WSe_2, can modify the properties of ZnO, enhancing its electrical and optical characteristics. This study investigates the effect of WSe_2 on the electronic properties and photovoltaic parameters of ZnO.

1. Experimental part. Methods and materials

In this study, zinc acetate ($Zn_5(OH)_8Cl_2$) was investigated. The modification of ZnO was carried out during sample preparation by introducing alcoholic solvents, specifically isopropanol (2-propanol), and by incorporating tungsten diselenide WSe_2 nanoparticles synthesized via laser ablation in a liquid medium.

For the fabrication of polymer solar cells, poly(3-hexylthiophene) (P3HT) was used as the electron donor, while the mono-adduct fullerene derivative indene - C_{60} ($IC_{60}MA$) served as the acceptor. In all experiments involving the preparation of thin films, high-purity chemical reagents were used, supplied by Ossila, Borun New Material Technology Co., Solaris Chem Ltd, Luminescence Technology Corp., and Sigma-Aldrich.

To fabricate the ZnO:NP WSe_2 nanocomposite film, WSe_2 nanoparticles were added to the ZnO solution in concentrations ranging from 2% to 10%. The amount of introduced nanoparticles was calculated based on their density using the following formula:

$$C_{NP} = \frac{C_{WSe2}}{m_{NP} \cdot N_A} = \frac{C_{WSe2}}{\rho_{WSe2} \cdot V_{NP} \cdot N_A} = \frac{\frac{m_{WSe2}}{V_{sol} M_{WSe2}}}{\rho_{WSe2} \cdot \frac{4\pi r^3}{3} \cdot N_A} \left(\frac{mol}{L}\right) \quad (1)$$

where: C_{NP} – the concentration of nanoparticles in the solution;
C_{WSe2} – the concentration of the substance in the solution before the laser ablation of WSe_2;
m_{NP} – the weight of an average nanoparticle;
N_A – Avogadro's number;
P_{WSe2}– the density of WSe_2;
V_{NP} – the volume of an average nanoparticle;
M_{WSe2} – weight of the target substance WSe_2;
V_{sol} – volume of solvent used in laser ablation;
M_{WSe2} – the molar mass of the substance is WSe_2;
r – the radius of the average nanoparticle.

ZnO:NPWSe_2 nanocomposite coatings were deposited on an FTO substrate using the spin-coating method at a speed of 4000 rpm. The samples were then subjected to thermal treatment at 150°C for 10 minutes to ensure the complete removal of residual solvent.

The current distribution on the surface of ZnO films with and without WSe_2 nanoparticles was measured using an Ntegra system (NT-MDT). The analysis was conducted in contact mode with a gold-coated HA_C/Au probe to map the current distribution. All measurements were performed under ambient conditions. ZnO films doped with WSe_2 nanoparticles at the highest concentration of 10% were used as samples. A critical challenge in this study was optimizing the scanning parameters, particularly selecting an appropriate probe.

2. Results and discussion

Figure 1 presents the experimental impedance spectra (depicted as data points) of organic solar cells (OSCs). In this model, R_1 corresponds to the equivalent resistance of the external electrodes R_{FTO} + $R_{ZnO:WSe2}$ + PEDOT:PSS + Ag), while the R_2C parameter characterizes the interface between the photoactive layer and ZnO:WSe_2 nanocomposite films.

Table 1 presents the obtained values of R_1, R_2 and C. As evident from the data, R_1 represents the total resistance of the external electrodes and the adjacent ETL and HTL layers. Since all functional layers, except ZnO:WSe_2, were fabricated under identical conditions, variations in R_1 are attributed to changes in the resistance of the ZnO:WSe_2 films. The lowest R_1 value is observed in the cell with the highest WSe_2 concentration.

The R_2 parameter, which characterizes recombination processes at the interface between the photoactive layer and ZnO:WSe_2 varies depending on the concentration of WSe_2 nanoparticles.

Since the films were fabricated under identical conditions, the changes in R_2 are attributed to the modification of the photoactive layer/ ZnO: WSe_2 interface. As shown in Table 1, an increase in the concentration of WSe_2 nanoparticles leads to a decrease in recombination resistance, indicating an enhancement of recombination processes.

Upon photoexcitation, electrons from the photoactive layer are injected into ZnO:WSe_2 and diffuse toward the external electrode. Simultaneously, the reverse process occurs, involving the recombination of electrons with holes in the photoactive layer. In most cases, recombination takes place through surface defect states in ZnO. Impedance spectroscopy also enables the determination of the time constant $\tau = RC$, which characterizes the charge carrier lifetime in ZnO:WSe_2.

With an increase in WSe_2 concentration up to 8%, a significant decrease in resistances R_1 and R_2 is observed, indicating improved material conductivity. This reduction is attributed to the optimal distribution of WSe_2 within ZnO, which enhances both structural integrity and electrical properties. However, at a concentration of 10%, the resistance increases again due to the aggregation of WSe_2 particles. The formation of large clusters leads to the emergence of defect zones,

disruption of material uniformity, and hindered charge transport, which adversely affects its conductivity and optoelectronic properties.

The analysis of the results revealed that at a nanoparticle concentration of 8% in the ZnO:WSe_2 composite film, optimal charge transport properties are achieved. At this concentration, the film resistance and charge carrier transfer resistance at the ZnO/electrode interface decrease by factors of 2 and 3.6, respectively, while the effective charge carrier mobility increases by a factor of 2.8. This indicates an optimal balance between nanoparticle distribution and material conductivity.

Figure 8 shows the impedance spectra of ZnO nanocomposite films ZnO:WSe_2. Data analysis shows that the introduction of WSe_2 into ZnO provides the best electric transport characteristics among the studied nanoparticles. At a concentration of 8%, the minimum values of film resistance and carrier transfer resistance are achieved, as well as the maximum charge mobility (table 1).

Figure 2 presents (a) the current-voltage characteristics of the organic solar cell with the FTO/ZnO:WSe_2/P3HT:IC60MA/Ag structure and (b) the architecture of the inverted PSC. ZnO nanocomposite films doped with WSe_2 nanoparticles were used as electron-selective electrodes in organic solar cells with a P3HT:IC60MA photoactive layer. The incorporation of WSe_2 into ZnO led to an improvement in Jsc and PCE compared to the reference device based on pure ZnO (table 2). The optimal performance was demonstrated by the device with an 8% WSe_2 concentration, where Jsc increased from 7.25 mA/см^2 to 9.29 mA/см^2, FF improved from 0.37 to 0.50 and PCE increased from 0.7% to 2.6%.

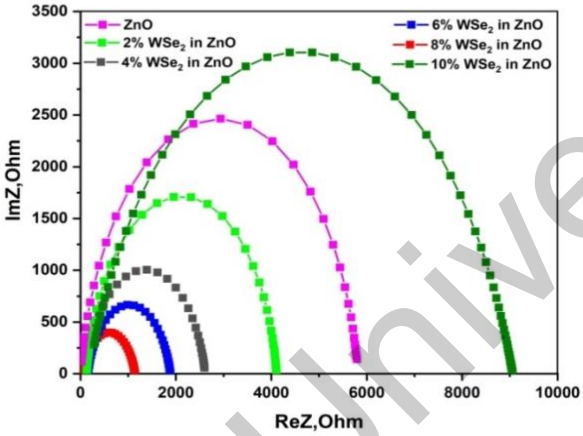

Fig.1. Effect of WSe_2 nanoparticles on ZnO film impedance spectra

Table 1. The value of the electrophysical parameters of ZnO:WSe_2 composite films

Sample	R_1, Om	R_2, Om	τ_D, c	Deff, ($cm^2 \cdot c^{-1}$)	μ, ($cm^2 \cdot V^{-1} \cdot c^{-1}$)
ZnO	131	5816	0,013	$2{,}2 \cdot 10^{-9}$	$0{,}8 \cdot 10^{-9}$
10μl (2%) WSe_2 in ZnO	120	3980	0,022	$3{,}2 \cdot 10^{-9}$	$2{,}0 \cdot 10^{-8}$
20μl (4%) WSe_2 in ZnO	117	2520	0,040	$7{,}2 \cdot 10^{-9}$	$2{,}8 \cdot 10^{-7}$
30μl (6%) WSe_2 in ZnO	109	1731	0,043	$6{,}7 \cdot 10^{-9}$	$2{,}6 \cdot 10^{-7}$
40μl (8%) WSe_2 in ZnO	101	1081	0,050	$5{,}8 \cdot 10^{-9}$	$2{,}2 \cdot 10^{-7}$
50μl (10%) WSe2 in ZnO	164	8932	0,032	$9{,}1 \cdot 10^{-9}$	$3{,}5 \cdot 10^{-7}$

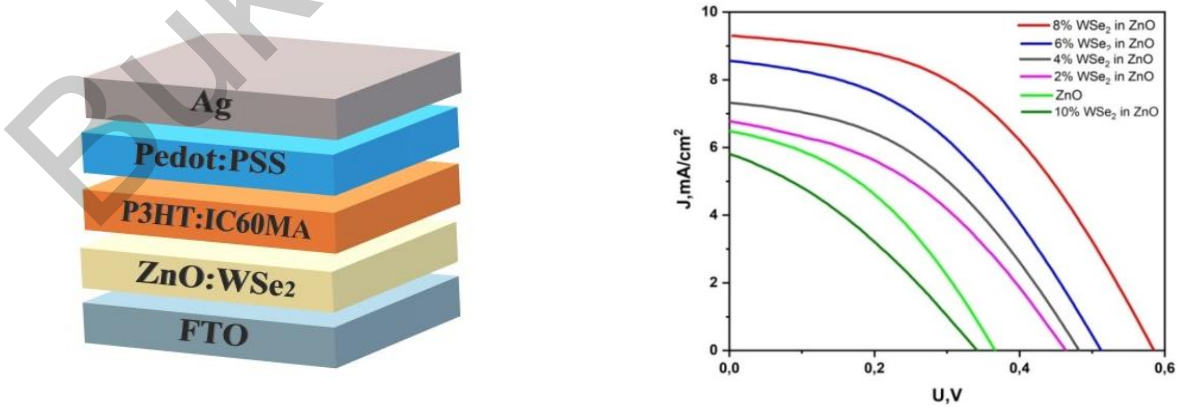

a) b)

Fig.2. (a) Current-voltage characteristics of the organic solar cell with the FTO/ZnO:WSe_2/P3HT:IC60MA/Ag structure; (b) the architecture of the inverted PSC.

Table 2. Photovoltaic characteristics of organic solar cells.

Sample	U_{oc} (B)	J_{sc} (мА/см^2)	U_{max}(B)	J_{max} (мА/см^2)	FF	PCE %
ZnO	0.27±0,01	7.25±0,05	0.27±0,01	4.07±0,05	0.37±0,01	0.7±0,05
10µl (2%) WSe_2 in ZnO	0.36±0,01	6.51±0,05	0.23±0,01	4.0±0,05	0.39±0,01	0.9±0,05
20µl (4%) WSe_2 in ZnO	0.46±0,01	6.84±0,05	0.27±0,01	5.7±0,05	0.48±0,01	1.5±0,05
30µl (6%) WSe_2 in ZnO	0.48±0,01	7.23±0,05	0.30±0,01	6.3±0,05	0.56±0,01	1.9±0,05
40µl (8%) WSe_2 in ZnO	0.58±0,01	9.29±0,05	0.38±0,01	7.2±0,05	0.50±0,01	2.6±0,05
50µl (10%) WSe_2 in ZnO	0.51±0,01	8.51±0,05	0.33±0,01	6.5±0,05	0.48±0,01	2.0±0,05

Conclusions

Technique for synthesizing WSe_2 nanoparticles via laser ablation in isopropanol has been developed. Nanocomposite ZnO films doped with WSe_2 nanoparticles were obtained within a concentration range of 2% to 10%. The absorption and impedance spectra of the composite films were measured. It was found that the incorporation of WSe_2 nanoparticles into ZnO reduces both the film resistance and charge carrier transfer resistance. A critical WSe_2 concentration of 8% was identified, at which the lowest resistance values and the highest efficiency of the polymer solar cell were achieved. Specifically, Jsc increased from 7.25 mA/cm^2 to 9.29 mA/cm^2, FF rose from 0.37 to 0.50, and PCE improved from 0.7% to 2.6%.

References

1 Vabbina P.K., Sinha R. (2017) Sonochemical synthesis of a zinc oxide core-shell nanorod radial p–n homojunction ultraviolet photodetector. *ACS Applied Materials & Interfaces*. 9(23), 19791-19799. https://doi.org/10.1021/acsami.7b03713

2 Chatzigiannakis G., Jaros A. (2020) Laser-microstructured ZnO/p-Si photodetector with enhanced and broadband responsivity across the ultraviolet−visible−near-infrared range. *ACS Applied Electronic Materials*. 2(9), 2819-2828. https://doi.org/10.1021/acsaelm.0c00538

3 Fang X., Bando Y. (2009) ZnO and ZnS nanostructures: ultraviolet-light emitters, lasers, and sensors. *Critical Reviews in Solid State and Materials Sciences*. 34(3-4), 190-223. https://doi.org/10.1080/10408430903245362

4 Nie S., Dastan D. (2020) Gas-sensing selectivity of n-ZnO/p-Co_3O_4 sensors for homogeneous reducing gas. *Journal of Physics and Chemistry of Solids*. 150, 109864. https://doi.org/10.1016/j.jpcs.2020.109864

5 Paracchino A., Laporte V. (2011) Highly active oxide photocathode for photoelectrochemical water reduction. *Nature Materials*. 10(6), 456-461. https://doi.org/10.1038/nmat3017

6 Nahm H.-H., Park C.H. (2014) Bistability of hydrogen in ZnO: origin of doping limit and persistent photoconductivity. *Scientific Reports*. 4, 4124. https://doi.org/10.1038/srep04124

УДК 661.632.26

ПЕРСПЕКТИВНЫЕ НАПРАВЛЕНИЯ ПЕРЕРАБОТКИ ШЛАКОВЫХ РАСПЛАВОВ

Серикбаев Б.Е., ЮКУ им. М. Ауэзова, г. Шымкент, Казахстан
Бажиров Н.С., ЮКУ им. М. Ауэзова, г. Шымкент, Казахстан
Бажиров Т.С., ЮКУ им. М. Ауэзова, г. Шымкент, Казахстан

При производстве многих видов продукций, связанных с высокотемпературными технологическими процессами, образуются значительные объемы шлаковых расплавов. К таким относятся процессы получения чугуна, стали, ферросплавов, фосфора электротермическим способом и другие. При этом объемы образующих шлаковых расплавов сопоставимы с объемами основного продукта. Уборка этого расплава и его утилизация является важной задачей металлургической и химической промышленности. Одно из главных направлений переработки шлаковых расплавов – грануляция непосредственно у печей (припечная грануляция). Наиболее распространена водная грануляция шлакового расплава, когда шлаковый расплав сливается в воду; при этом объем воды превышает объем шлака до десяти раз. Полученная пульпа затем обезвоживается и полученный гранулированный шлак отвозится в отвалы или отгружается потребителю. Полученный шлак используется при производстве строительных материалов. Еще одним способом переработки шлаковых расплавов является метод «намораживания» или сухой способ грануляции. Сравнивая вышеуказанные способы, необходимо отметить, что водная грануляция является более надежным способом переработки шлаковых расплавов. Технология и оборудование, используемые в настоящее время для получения гранулированных шлаков, не отвечают современным требованиям по качеству продукции, уровню механизации и автоматизации производственных процессов, условиям труда обслуживающего персоналаи, что особенно недопустимо, требованиям по защите окружающей среды от загрязнений. Гранулированные шлаки,